8-1-2015

Structure-Based Screen Identifies a Potent Small Molecule Inhibitor of Stat5a/b with Therapeutic Potential for Prostate Cancer and Chronic Myeloid Leukemia.

Zhiyong Liao
Thomas Jefferson University, zhiyong.liao@jefferson.edu

Lei Gu
Thomas Jefferson University, lei.gu@jefferson.edu

Jenny Vergalli
Thomas Jefferson University, jenny.vergalli@jefferson.edu

Samanta A. Mariani
Thomas Jefferson University, samanta.mariani@jefferson.edu

Marco De Dominici
Thomas Jefferson University, Marco.DeDominici@jefferson.edu

See next page for additional authors

Authors
Zhiyong Liao, Lei Gu, Jenny Vergalli, Samanta A. Mariani, Marco De Dominici, Ravi K. Lokareddy, Ayush Dagvadorj, Puranik Purushottamachar, Peter A. McCue, Edouard J. Trabulsi, Costas D. Lallas, Shilpa Gupta, Elyse Ellsworth, Shauna Blackmon, Adam Ertel, Paolo Fortina, Benjamin E. Leiby, Guanjun Xia, Hallgeir Rui, David T. Hoang, Leonard G Gomella, Gino Cingolani, Vincent Njar, Nagarajan Pattabiraman, Bruno Calabretta, and Marja T. Nevalainen

HHS Public Access

Author manuscript

Mol Cancer Ther. Author manuscript; available in PMC 2016 August 01.

Published in final edited form as:

Mol Cancer Ther. 2015 August ; 14(8): 1777–1793. doi:10.1158/1535-7163.MCT-14-0883.

Structure-based screen identifies a potent small-molecule inhibitor of Stat5a/b with therapeutic potential for prostate cancer and chronic myeloid leukemia

Zhiyong Liao[1], **Lei Gu**[1], **Jenny Vergalli**[1], **Samanta A. Mariani**[1], **Marco De Dominici**[1], **Ravi K. Lokareddy**[2], **Ayush Dagvadorj**[1], **Puranik Purushottamachar**[3,*], **Peter A. McCue**[4], **Edouard Trabulsi**[5], **Costas D. Lallas**[5], **Shilpa Gupta**[1,6,*], **Elyse Ellsworth**[1], **Shauna Blackmon**[1], **Adam Ertel**[1], **Paolo Fortina**[1], **Benjamin Leiby**[7], **Guanjun Xia**[1], **Hallgeir Rui**[1,4,6], **David T. Hoang**[1], **Leonard G. Gomella**[5], **Gino Cingolani**[2], **Vincent Njar**[3,*], **Nagarajan Pattabiraman**[1,8], **Bruno Calabretta**[1], and **Marja T. Nevalainen**[1,5,6]

[1]Department of Cancer Biology, Sidney Kimmel Cancer Center (SKCC), Thomas Jefferson University, Philadelphia, PA

[2]Department of Biochemistry, SKCC, Thomas Jefferson University, Philadelphia, PA

[3]School of Pharmacy; SKCC, Thomas Jefferson University, Philadelphia, PA

[4]Department of Pathology, SKCC, Thomas Jefferson University, Philadelphia, PA

[5]Department of Urology, SKCC, Thomas Jefferson University, Philadelphia; PA

[6]Department of Medical Oncology, SKCC, Thomas Jefferson University, Philadelphia, PA

[7]Division of Biostatistics, Department of Pharmacology and Experimental Therapeutics, SKCC, Thomas Jefferson University, Philadelphia, PA

[8]Department of Oncology, Lombardi Comprehensive Cancer Center, Georgetown University, Washington, District of Columbia

Abstract

Bypassing tyrosine kinases responsible for Stat5a/b phosphorylation would be advantageous for therapy development for Stat5a/b-regulated cancers. Here, we sought to identify small-molecule inhibitors of Stat5a/b for lead optimization and therapy development for prostate cancer (PC) and Bcr-Abl-driven leukemias. *In silico* screening of chemical structure databases combined with medicinal chemistry was used for identification of a panel of small-molecule inhibitors to block SH2-domain-mediated docking of Stat5a/b to the receptor-kinase complex and subsequent

Address correspondence to: Marja T. Nevalainen, MD, PhD, Dept. of Cancer Biology, Medical Oncology, Urology, Kimmel Cancer Center, Thomas Jefferson University, 233 S. 10th Street, BLSB 309, Philadelphia, PA 19107. marja.nevalainen@jefferson.edu Tel: 215-503-9250, Fax: 215-503-9245.

*Current address:

Vincent C. O. Njar, PhD, Professor of Medicinal Chemistry and Pharmacology, Dept. of Pharmacology;, Head, Medicinal Chemistry Group, Center for Biomolecular Therapeutics;, Member, Greenebaum Cancer Center, University of Maryland School of Medicine, 685 West Baltimore Street; HSF 1, Suite 580E; Baltimore, MD 21201, USA, Tel: 410-706-6364 (Baltimore), E-mail: vnjar@som.umaryland.edu

Puranik Purushottamachar, PhD, University of Maryland School of Medicine, 685 West Baltimore Street; HSF 1, Suite 580E; Baltimore, MD 21201, USA, p.purushottamahar@som.maryland.edu

Shilpa Gupta, MD; Medical Oncology, Moffitt Cancer Center; 12902 Magnolia Drive, Tampa, FL 33612; shilpa.gupta@moffitt.org

phosphorylation and dimerization. We tested the efficacy of the lead-compound, IST5-002, in experimental models and patient samples of two known Stat5a/b-driven cancers, prostate cancer (PC) and chronic myeloid leukemia (CML). The lead compound Inhibitor of Stat5-002 (IST5-002) prevented both Jak2 and Bcr-Abl-mediated phosphorylation and dimerization of Stat5a/b, and selectively inhibited transcriptional activity of Stat5a (IC_{50} 1.5 μM) and Stat5b (IC_{50} 3.5 μM). IST5-002 suppressed nuclear translocation of Stat5a/b, binding to DNA and Stat5a/b target gene expression. IST5-002 induced extensive apoptosis of PC cells, impaired growth of PC xenograft tumors and induced cell death in patient-derived PCs when tested *ex vivo* in explant organ cultures. Importantly, IST5-002 induced robust apoptotic death not only of imatinib-sensitive but also imatinib-resistant chronic myeloid leukemia (CML) cell lines and primary CML cells from patients. IST5-002 provides a lead structure for further chemical modifications for clinical development for Stat5a/b-driven solid tumors and hematological malignancies.

Keywords

Stat5a/b; small molecular inhibitor; SH2 domain; prostate cancer; leukemia

Introduction

There is an unmet medical need for pharmacological inhibitors of Signal Transducer and Activator of Transcription 5a/b (Stat5a/b). Stat5a/b is critical for growth and progression of solid tumors and hematologic malignancies, specifically prostate cancer (PC) (1–9) and Bcr-Abl-driven leukemias (10–19), respectively. In PC, effective therapeutic options are lacking for advanced castration-resistant PC (CRPC), for which Stat5a/b is an experimentally established therapeutic target candidate (2, 4, 9, 20, 21). Multiple findings support Stat5a/b as a therapeutic target protein in PC: 1) inhibition of Stat5a/b expression or activation induces rapid apoptotic PC cell death (1–3, 9, 22); 2) blockade of Stat5a/b signaling inhibits growth of both primary PC and CRPC (2, 4, 5, 9, 21–23); 3) Stat5a/b promotes epithelial-mesenchymal transition (EMT) and metastasis of human PC (5); 4) the Stat5a/b gene locus is frequently amplified in clinical PCs during progression to metastatic CRPC (6); 5) Stat5a/b activation in PC predicts early recurrence and PC-specific death (7, 8, 21).

CML is a clonal hematopoietic stem cell malignancy characterized by the unique t(9:22)(q34:q11) translocation, which generates the *BCR-ABL* oncogene (24). Bcr-Abl is a constitutively active tyrosine kinase promoting transformation, proliferation and survival of CML cells via Stat5a/b signaling (10–19, 25). Resistance to the predominant pharmacological inhibitor of Bcr-Abl, imatinib mesylate (Gleevec®) (26), induced by point mutations within the Abl kinase domain or overexpression of Bcr-Abl (27, 28), is, in part, dependent on activation of the Stat5a/b signaling pathway (10, 14, 18).

Stat5a/b includes two highly homologous isoforms Stat5a and Stat5b (hereafter referred to as Stat5a/b), which display >90% amino acid identity and are encoded by genes juxtaposed on chromosome 17q21.2 (29). Stat5a/b are latent cytoplasmic proteins that function as both signaling proteins and nuclear transcription factors. Activation of Stat5a/b occurs through inducible phosphorylation of a conserved C-terminal tyrosine residue (29). Phosphorylated

Stat5a/b (pY694/699) molecules form functional parallel dimers that translocate to the nucleus and bind specific DNA response elements (29). Stat5a/b proteins comprise five functional domains: 1) N-terminal domain (29); 2) coiled-coil domain (30); 3) DNA-binding domain (29); 4) Src-homology 2 (SH2)-domain, which mediates receptor-specific recruitment and Stat5a/b dimerization (29); and 5) C-terminal transactivation domain (29). In PC, Stat5a/b is activated by the upstream kinase Jak2 and by other tyrosine kinases such as Src and growth factor receptors (31–34). In CML, Stat5a/b is phosphorylated directly by Bcr-Abl (35) and targeting Stat5a/b would bypass Bcr-Abl and might provide an effective therapy especially in imatinib-resistant CML (10–19, 25). Therefore, targeting of Stat5a/b as a cytoplasmic signaling protein in both PC and CML may prove a more effective therapeutic strategy than inhibiting Stat5a/b tyrosine kinases.

In the present work, we identified a small-molecule inhibitor family of Stat5a/b through structure-based *in-silico* screening and medicinal chemistry by targeting the Stat5a/b SH2-domain. The SH2-domain of a Stat5 monomer docks transiently to a phospho-tyrosyl moiety of a tyrosine kinase complex, which facilitates phosphorylation of Y694/699 residue of Stat5a/b. The SH2-domain of each phosphorylated Stat5 monomer forms transcriptionally active parallel dimers through binding of pY694/699 residue of the partner Stat5 monomer (36). Therefore, a small molecule which interferes with the SH2-domain should inhibit both Stat5a/b phosphorylation and dimerization. Our lead compound, Inhibitor of Stat5-002 (IST5-002) blocked both Jak2 and Bcr-Abl-mediated phosphorylation of Stat5a/b and disrupted dimerization, nuclear translocation, DNA binding and transcriptional activity. IST5-002 induced apoptotic death of PC cells and imatinib-sensitive and -resistant CML cells *in vitro*. Furthermore, IST5-002 inhibited growth of PC xenograft tumors *in vivo* and Stat5a/b-positive patient-derived PCs in *ex vivo* organ culture. These findings establish a potent small-molecule Stat5a/b inhibitor compound for further optimization and therapy development for PC and Bcr-Abl-driven leukemias.

Methods

Discovery of small-molecule Stat5 inhibitor IST5-002 through *in-silico* database screen

To identify candidate compounds that disrupt Stat5a/b dimerization by targeting the SH2-domain, we created a three-dimensional model of the SH2-domain dimer structure (amino acid residues 589–710) of human Stat5b using the homology modeling software, MODELLER 6v2. The sequence of the human Stat5b SH2-domain with an additional 14 amino acids (697-DGYVKPQIKQVVPE-710) at the C-terminus, containing the phosphotyrosine (UniProtKB/Swiss-Prot ID:P51692), was used to search for sequences that matched the sequences of three-dimensional structures of proteins and their complexes available in the Protein Data Bank using BLAST (National Center for Biological Information). The sequence homology between human *STAT5A* and *STAT5B* is approximately 92%, whereas the sequence homology between the SH2-domains of human *STAT5A* and *STAT5B* is approximately 98% (29). We identified two protein structures: 1) Stat3-DNA complex (PDB ID: 1BG1) (30), with identities equal to 35%, positives equal to 11% and gaps equal to 53%); and 2) tyrosine-phosphorylated Stat1-DNA complex (PDB ID: 1BF5) (37), with identities equal to 56%, positives equal to 34% and gaps equal to 12%)

with expected values (e-value) of 9e-14 and 7e-12, respectively. By aligning the sequences between the SH2-domains of human *STAT5B* and *STAT3* and using the crystal structure of the SH2 domain of the Stat3-DNA complex as a template, a homology model of the SH2-domain of human Stat5b was built. This homology model was further energy-minimized until the root-mean-square deviation was < 0.09 using AMBER7 (UCSF) and its force field with a distance-dependent dielectric constant. To perform structure-based *in-silico* screening, the pY binding subpocket is insufficient to identify potent inhibitors against the dimer of SH2-domains, requiring additional two to three subpockets near the pY binding pocket. From analysis of the crystal structure of the Stat1-DNA complex at the SH2 dimer interface, it is clear that additional subpockets are available both at the N and C-termini of the pY-binding site at the dimer interface. In order to identify these additional subpockets, 64 oligopeptides derived from the tetrapeptide sequence pYVKP (where pY is the phosphorylated tyrosine) by varying the amino acids to all eight hydrophobic/aromatic acids independently both at the second and fourth amino acid positions and docked into the binding site on the SH2-domain. By calculating the interaction energies of all 64 amino acids and rank-ordering them, we selected the following residues of Stat5b as the binding sites for *in-silico* screening: 600K, 604H, 618-RFSDSEIGG-626, 628T, 638-RMFWNLMPF-646, 707-VVPE-710.

In-silico screening of small organic molecules from databases (NCI, Maybridge, LeadQuest, Virtual Chemistry and Drug-Like Compounds, http://www.chemnavigator.com) of 30 million compounds was performed against the subpockets at the dimer interface for their ability to disrupt Stat5b dimerization (Fig. 1a, b, c). We wanted to identify compounds that would mimic the side chain of pY and have additional groups occupying the subpockets described above. In our first level search, we identified compounds with free phosphate group attached either to an aromatic or aliphatic five or six-member ring. These compounds were screened against the phosphotyrosine-binding pocket using a flexible ligand docking program (FlexX module of Sybyl, Tripos) and multiple scoring functions (molecular mechanics energy, surface area, etc.), which led to the selection of the top-ranking 100 compounds. These compounds, along with their protein complexes, were energy-minimized using molecular mechanics CFF91 force-filed to better fit the ligands into the binding pocket. The top-ranking 30 small-molecule inhibitors were selected from visual analysis of docking position and interactions to be further validated in biological assays, and as the basis of the design and synthesis of compound analogs (Supplementary Fig. 1).

Cell lines and reagents

PC-3, DU145 and LNCaP PC cells, T47D breast cancer cells, and CML-cells (KCL22, K562 and BV173) (all from ATCC in 2002), were cultured in RPMI 1640 (Mediatech) containing penicillin (50 IU/ml)/streptomycin (50 μg/ml) (Mediatech) and 10% fetal bovine serum (FBS; Gemini BioProducts). CWR22Rv1 cells were provided by Dr. Thomas Pretlow (Casewestern Reserve University) in 2004. K562, imatinib-resistant K562 (K562R), BV173, imatinib-resistant-BV173 (BV173T315I) were maintained in IMDM (Mediatech) supplemented with 1% penicillin/streptomycin, L-glutamine and 10% FBS. KCL22R, K562R and BV173R were kindly provided by Dr. Nicholas J. Donato (2009, Univ. of Michigan). SUP-B15, 12878 and 3798 (2009, Coriell Institute) were maintained in Iscove's

medium with 10% FBS. LNCaP cells were supplemented with 0.5 nM dihydrotestosterone (DHT; Sigma-Aldrich). CML CD34+ cells from three CML patients (#3-342, #9537, #3-295) (2010, a gift from Dr. Tessa Holyoake, Univ. of Glasgow, Scotland, UK) were maintained in SFEM (Stem Cell Technologies) supplemented with 1% penicillin/streptomycin and L-glutamine (Gibco), a cytokine cocktail (100 ng/ml Flt3 ligand, 100 ng/ml SCF, 20 ng/ml IL-3 and 20 ng/ml IL-6 (Stem Cell Technologies) and 100 ng/ml rhTPO (Prospec). Monkey kidney fibroblast (COS-7), human lung cancer (A549), fibrosarcoma (HT1080), pancreatic cancer (CAPAN) and liver cancer (HepG2) cell lines (all from ATCC in 2008) were grown in DMEM (Invitrogen, Grand Island, NY) supplemented with 10% FBS, 2 mM L-glutamine, and penicillin-streptomycin (Mediatech). All cell lines included in this study have been authenticated on a regular basis in the users' laboratory. The testing has been conducted by,DNA fingerprinting, isozyme collection, observation of characteristic cell morphology, hormone/growth factor responsiveness and the expression of cell lines specific markers such as PSA, hormone receptors, Stat3/Stat5, Erk1/2Protein, BCR-Abl. All cell lines were tested for mycoplasma contamination (PCR Mycoplasma Detection Set; Takara Bio Inc.,) every 3 months. Pimozide was obtained from Sigma Aldrich.

Luciferase reporter gene assays

PC-3 cells (2×10^5) were transiently co-transfected with 0.25 μg of pStat5a or pStat5b and pPrlR (prolactin receptor), 0.5 μg of p-beta-casein-luciferase (beta-casein-Luc) and 0.025 μg of pRL-TK (*Renilla luciferase*). After 24 h, cells were serum-starved for 10 h, pretreated with compounds at indicated concentrations for 1 h, and stimulated with 10 nM human prolactin (hPrl) for 16 h. For determination of Stat3 transcriptional activity, 0.25 μg of pcDNA-Stat3, 0.25 μg of pcDNA-IL6-R, 0.5 μg of pStat3-luciferase (Panomics) and 0.025 μg of pSV-β-Gal (Promega) were co-transfected to LNCaP cells, followed by serum-starvation and stimulation with 50 ng/ml IL-6 (Prospec) for 16 h. Cell lysates were assayed for firefly and *Renilla* luciferase activities using the dual-luciferase reporter assay system (Promega), as described previously (23).

Protein solubilization, immunoprecipitation and immunoblotting

Cell pellets were immunoprecipitated and immunoblotted as described previously (2, 3, 5, 23). Stat5a, Stat5b and Jak2 were immunoprecipitated from whole cell lysates with anti-Stat5a, anti-Stat5b (4 μl/ml; Millipore, Billerica, MA) or anti-Jak2 (Millipore) pAbs. For immunoblotting, primary antibodies were used at the following concentrations: anti–phosphotyrosine-Stat5a/b (Y694/Y699) mAb (1 μg/ml, Advantex BioReagents), anti-Stat5ab mAb (1:250; BD Biosciences), anti-c-Abl mAb (1:500, Calbiochem), anti-Grb2 mAb (5:100, BD Biosciences), anti-β-actin pAb (1:4,000; Sigma), anti-cyclin D1 mAb (1:1000, BD Biosciences), anti-pPAK1/2 (1:1000, Cell Signaling), anti-Bcl-xL pAb (1:1000, Cell Signaling) and anti-phosphotyrosine mAb (1:1000, Millipore).

Cell-based immunoassay for tyrosine-phosphorylated Stat5a/b

T47D cells in 96-well plates were serum-starved for 16 h, pretreated with IST-002 at the indicated concentrations for 2 h, followed by stimulation with hPrl (2 nM) for 15 min, and

fixation in 20°C acetone/methanol followed by incubation with anti-pStat5a/b rabbit mAb (1:200; Cell Signaling) and secondary HRP-conjugated anti-rabbit Ab (1:2000, Cell Signaling). The amount of phospho-Stat5a/b was evaluated using one-step Ultra TMB substrate (Thermo Scientific) at 450 nm. Cells cultured in the absence of IST-002 and treated with or without prolactin served as positive and negative controls, respectively. The inhibition curve and IC50 were derived from triplicate measurements using Sigmaplot.

Kinase Activity Assay

Inhibitory activity of IST5-002 was tested against a panel of 50 kinases using KinaseSeeker Technology (Luceome Biotechnologies, Tuscon, AZ). Prior to initiating the kinase profiling, IST5-002 was evaluated for false positive activity against split-luciferase. For the kinase assays, each Cfluc-Kinase was translated along with Fos-Nfluc using a cell-free system (rabbit reticulocyte lysate) at 30 C for 90 min. An aliquot (24 μL) of this lysate containing either 1 μL of DMSO (for no-inhibitor control) or compound solution in DMSO (1 μM final concentration) was incubated for 30 minutes at room temperature followed by 1 hour in the presence of a kinase specific probe. 80 μL of luciferin assay reagent was added to each solution and luminescence was immediately measure in a luminometer. Profiling data for all kinases was plotted as % activity remaining vs. kinases profiled.

Determination of Stat5a dimerization by co-immunoprecipitation

The dimer formation of Stat5a was analyzed as described previously (4) and in the Supplementary Methods. Cells were serum-starved for 16 h, followed by pre-treatment with IST5-002 or the control compound (Ctrl) for 2 h at indicated concentrations, and stimulated with hPrl (10 nM) in serum-free medium for 30 min. Whole cell lysates were immunoprecipitated with anti-Myc mAb (2 μg/sample; Santa Cruz Biotechnology) and immunoblotted with anti-Flag mAb (1:1000; Genomics), anti-Myc mAb (1:1000; Santa Cruz Biotechnology) and anti-actin pAb (1:4000, Sigma-Aldrich).

Generation of adenoviral vectors for gene delivery of Stat5 and PrlR

pcDNA-CMV-WT-*STAT5A* and pcDNA-CMV-constitutively active *STAT5A* (CAStat5a) (Stat5aS710F) (38) were cloned to adenoviral vector using BD Adeno-X™ Expression System 2 (BD Biosciences Clontech). pcDNA-CMV-WT-*STAT5A* and pcDNA-CMV-constitutively active *STAT5A* (CAStat5a) (Stat5aS710F) (5) were cloned to adenoviral vector using BD Adeno-X™ Expression System 2 (BD Biosciences Clontech) according to the manufacturer's protocol. The purified recombinant adenovirus was linearized by *Pac*I digestion and transfected to QBI-293A cells (Qbiogene) to produce infectious recombinant adenoviruses. The resulting AdWTStat5a, AdCAStat5a and AdPrlR primary viral stocks were expanded in large-scale cultures, purified by double cesium chloride gradient centrifugation, and titrated by a standard plaque assay method in QBI-293A cells, as per the manufacturer's instructions.

Immunofluoresence cytochemistry of Stat5a/b and Stat3

PC3 cells were infected with AdWTStat5a and AdPrlR at MOI 4. Serum-starved (10 h) cells were pretreated with IST5-002 or control compound (2 h) and stimulated with 10 nM Prl (30

min). For analysis of IST5-002 efficacy in inhibition of Stat3 nuclear translocation, DU145 cells were serum-starved, pretreated with IST5-002, AZD1480 or vehicle at indicated concentrations for 2 h, before cells were stimulated with IL-6 (ProSpec-Tany Technogene) at 5 nM (30 min). Fixed cells were incubated with rabbit anti-Stat5 pAb (1:200; Santa Cruz Biotechnology) or anti-pYStat3 pAb (1:100; Cell Signaling), followed by goat anti-rabbit fluorescein IgG (1:200; Vector Laboratories), as described previously (23).

Electrophoretic mobility shift assay (EMSA)

EMSA assays were conducted as we have described previously (23).

Cell viability and DNA fragmentation assay

Cell viability was determined by Cell Titer 96® Aqueous Assay kit (Promega). The number of living cells was also determined by counting the attached vs. non-attached cells using a hemacytometer and trypan blue exclusion. DNA fragmentation was analyzed by photometric enzyme immunoassay according to the manufacturer's instructions (Cell Death Detection ELISA^{PLUS}; Roche).

Caspase-3 activation assay

CWR22Rv1 cells were treated with IST5-002 (12.5 μM) or vehicle for indicated periods of time. Caspase-3 was captured by anti-caspase-3 mAb, followed by caspase-3-mediated enzymatical cleavage of 7-amino-4-trifluoromethyl-coumarin (AFC) substrate measured at 505 nm. In Stat5a/b rescue experiments, CAStat5a was expressed using an adenoviral vector (MOI=2) 6 h prior to treatment of cells with IST5-002 (12.5 μM) or vehicle for 72 h.

Cell cycle analysis

Cells were treated with IST5-002, vehicle or control compound for 24, 48 and 72 h, fixed and stained with propidium iodide (PI) and RNase A (Sigma-Aldrich). PI fluorescence intensity was analyzed by a flow cytometer using FL-2 channel.

Colony formation assay

CML-blast crisis lines and CML CD34+ primary cells were plated in the presence of DMSO, 5 μM IST-002 or 5 μM control compound. After 3 h incubation, 1 x 10^3(K562), 2.5 x 10^3 (BV173 and KCL22) or 3 x 10^4 (CML) cells were plated in duplicate in methylcellulose and the number of colonies was assessed 5–10 days after plating.

RNA expression profiling

RNA from vehicle, IST5-002, scramble shRNA, and Stat5a/b-shRNA was profiled in triplicate using the Affymetrix GeneChip Human Gene 1.0 ST microarray platform. Differential gene expression comparisons were performed for IST5-002 vs. vehicle, and Stat5a/b-shRNA vs. scramble-shRNA using a t-test with false discovery rate correction. Protocols for RNA preparation, hybridization, scanning, and statistical analysis are described in detail in the Supplementary Methods. The accession number for the sDNA array data is GSE61312.

Human prostate cancer xenograft tumor growth studies

Castrated male athymic nude mice were purchased from Taconic and cared for according to the institutional guidelines. Mice were implanted with sustained-release dihydrotestosterone (DHT) pellets (60-day release, 1 pellet/mouse, Innovative Research of America) 3 days before PC cell inoculation. Briefly, 1.5×10^7 CWR22Rv1 cells were mixed with 0.2 ml of Matrigel (BD Biosciences), and inoculated subcutaneously (s.c.) into flanks of nude mice (one tumor/mouse) as described previously (2–4). After one week, tumor sizes were measured, and mice were randomly distributed into five groups (10 mice/group). Mice were treated daily for 10 days by intraperitoneal (i.p.) injections with 0.2 ml of IST5-002 dissolved in 0.3% hydroxypropyl cellulose (HPC, Sigma-Aldrich) at 25 mg/kg, 50 mg/kg or 100 mg/kg body weight, or with 0.2 ml 0.3% HPC solution, or no treatment, and tumor sizes were measured three times per week. Tumor volumes were calculated using the following formula: 3.14 × length × width × depth/6. When the tumors reached 15–20 mm in diameter in the control groups, mice were sacrificed and tumor tissues were harvested. Percent changes in tumor volume of each group are presented.

Ex vivo organ culture testing of Stat5-inhibitor efficacy in clinical prostate cancers

PC specimens were obtained from patients with localized or locally advanced PC undergoing radical prostatectomy and bilateral iliac lymphadenectomy (Table 1). The Thomas Jefferson University Institutional Review Board approved this work to be in compliance with federal regulations governing research on deidentified specimens [45 CFR 46.102(f)]. A zero-sample prior to organ culture of each individual PC was formalin-fixed for the analysis of nuclear Stat5a/b status. Prostate organ cultures were performed as described earlier (4, 7, 34, 39) and in the Supplementary Methods section.

Stat5a/b immunohistochemistry and TUNEL assay of paraffin-embedded tissue sections

Immunohistochemistry (IHC) staining of Stat5a/b and TUNEL assay were performed as described previously (1, 3–5, 7, 8, 21). Viable, active nuclear Stat5a/b-positive, Stat3-positive or apoptotic (fragmented DNA) cells vs. total number of cells (viable and dead) were counted for 3 views/tumor and 1 view covering each organ culture explant (20–25 explants per treatment group per patient) and expressed as percentages, as demonstrated previously (4). The average cell number per explant is determined of a sample of each patient prior to culture. All percentages within each treatment group (tumor or organ culture explant) were averaged.

Statistical analyses

Mixed-effects linear regression was used to model log 10-transformed tumor volumes. A quadratic curve in time was modeled separately for each treatment group. Random terms were included for the intercept, slope, and quadratic effect, allowing for each animal's curve to differ from the mean curve in its group. Differences in the groups with respect to the geometric mean tumor volume at days 1, 3, 6, 8 and 10 were tested, and at day 10, pairwise comparisons were performed to identify which groups differed from each other. P-values were adjusted using Bonferroni's method. $P<0.05$ was considered significant.

For tumor cell viability and nuclear Stat5 or Stat3 levels, analysis of variance implemented in SAS ProcMIXED was used to test for differences in responses across groups. Pairwise comparisons were performed to compare each inhibitor dose to the control groups and p-values for pairwise comparisons were adjusted using the Bonferroni method.

For cancer cell viability and nuclear Stat5 content in organ explant cultures, mixed-effects linear regression was used for statistical analysis of responders, followed by pairwise comparisons adjusted using the Bonferroni method. For non-responders, Kruskal-Wallis test was utilized due to the small number of measurements for each group.

Results

Virtual screen identifies a small-molecule inhibitor of Stat5a/b phosphorylation and dimerization

To identify a family of Stat5a/b inhibitor compounds, we used *in-silico* structure-based screening and medicinal chemistry. Docking of the most promising compound, Inhibitor of Stat5-002 (IST5-002), to the binding site of the Stat5b SH2-domain is depicted (Fig. 1a, b, c). Chemical structures of IST5-002 (MW 437 Da), a randomly selected control compound (Ctrl) of similar molecular weight (343 Da) (Fig. 1d) and other IST5-family members (Supplementary Fig. 1) are shown.

To determine if IST5-002 blocks Stat5a/b transcriptional activity, PC-3 cells were co-transfected with prolactin receptor (PrlR), Stat5a or Stat5b, and a Stat5a/b-luciferase reporter (β-casein-luciferase). Cells were treated with IST5-002 or Ctrl for 2 h prior to and during Stat5a/b activation by stimulation with human prolactin (hPrl, 10 nM; 16 h). IST5-002 robustly inhibited transcriptional activity of Stat5a (IC_{50} = 1.5 μM) and Stat5b (IC_{50} = 3.5 μM) in a dose-dependent manner, compared to Ctrl (Fig. 1e). Design and synthesis of IST5-002 analogs and structure-activity-relationship (SAR) studies (Supplementary Table 1) identified a family of IST5-002 inhibitors (Supplementary Fig. 1) which displayed efficacies comparable to IST5-002.

To analyze if IST5-002 suppresses formation of transcriptionally active phosphorylated dimers, Bcr-Abl-positive K562 cells were treated with increasing concentrations of IST5-002 (3 h), using pimozide (15) and Ctrl as positive and negative controls, respectively. Remarkably, IST5-002 blocked Bcr-Abl-induced Stat5a/b phosphorylation at 5 μM (Fig. 1f). At the same time, pimozide, a previously reported Stat5a/b inhibitor (15), required 20–40 μM to fully block Stat5a/b phosphorylation under these same conditions. However, pimozide is likely to induce a number of off-target effects related to the high concentrations needed for Stat5a/b inhibition. IST5-002 did not affect Bcr-Abl tyrosine phosphorylation levels in K562 cells (Fig. 1f). Next, serum-starved CWR22Rv1, HC-11 and T47D cells were treated with IST5-002 (2 h), followed by stimulation with hPrl (30 min). For CWR22Rv1 (Fig. 1g) and HC-11 (Supplementary Fig. 2a) cells, Stat5a/b were immunoprecipitated and immunoblotted with anti-pYStat5a/b antibody (Fig. 1g), while a cell-based immunoassay was used to monitor Stat5a/b phosphorylation in T47D cells (Supplementary Fig. 2b). IST5-002 blocked phosphorylation of Stat5a/b (CWR22Rv1, IC_{50}=22 μM; HC-11, IC_{50}=12 μM; T47D, IC_{50}=24.8 μM), while total Stat5a/b levels remained unaffected. Phosphorylation

of Jak2 was unaffected by IST5-002, indicating that IST5-002 does not inhibit Jak2 (Fig. 1g). Moreover, kinase activity profiling assay indicated no specific inhibition of other kinases in a panel of 50 kinases by IST5-002 (Supplementary Fig. 3) including activity of PAK1/2 (40) (Supplementary Fig. 4). To test if IST5-002 disrupts dimerization of Stat5a/b, we generated and co-transfected *FLAG*- and *MYC*-tagged Stat5a into PC-3 cells along with PrlR. Serum-starved cells were treated with IST5-002 or Ctrl before stimulation with hPrl (10 nM) (30 min). Lysates were immunoprecipitated with anti-Myc antibodies and immunoblotted with anti-Flag or anti-Myc antibodies. As expected, hPrl stimulation induced Stat5a dimerization, which was inhibited by IST5-002 (IC_{50} = 11 μM) (Fig. 1h). We conclude that IST5-002 effectively blocks molecular events associated with Stat5a/b activation, including phosphorylation, dimerization and transcriptional activity.

IST5-002 suppresses downstream signaling events and target gene expression induced by Stat5a/b in PC and CML cells

We next investigated if IST5-002 disrupts downstream signaling events induced by Stat5a/b activation. To assess if nuclear translocation of Stat5a/b is impacted, we expressed Stat5a and PrlR in PC-3 cells and treated serum-starved cells with IST5-002 (2 h), prior to stimulation with hPrl (10 nM) (30 min). In the absence of hPrl, Stat5a was predominantly localized in the cytoplasm, as demonstrated by immunocytochemistry (Fig. 2a). Addition of hPrl robustly induced Stat5a nuclear translocation, which was abrogated by IST5-002 at 15 μM (Fig. 2a).

To determine if IST5-002 inhibits DNA binding of activated Stat5a/b, we employed electrophoretic mobility shift assay (EMSA) using the Stat5a/b response element of the beta-casein gene promoter as a probe (Fig. 2b). COS-7 cells transfected with PrlR and Stat5a were serum-starved and pre-treated with IST5-002 (2 h), followed by hPrl stimulation (10 nM) (30 min). As predicted, IST5-002 reduced binding of Stat5a/b to its DNA target sequence by approximately 50% at 25 μM, compared to Ctrl-treated cells (Fig. 2b).

To evaluate specificity of IST5-002 for Stat5a/b, we tested the ability of IST5-002 to inhibit nuclear translocation and transcriptional activity of interleukin-6 (IL-6)-induced Stat3. Serum-starved DU145 cells were pretreated with IST5-002 or a positive control compound, Jak2 inhibitor AZD1480 (4, 41), before stimulation with IL-6 (5 nM). While AZD1480 effectively suppressed Stat3 nuclear translocation, IST5-002 had no demonstrable effect, even at a higher concentration (50 μM) (Fig. 2c). We reconstituted the IL-6-receptor-Stat3 signaling pathway in LNCaP cells and introduced a Stat3-luciferase reporter. Serum-starved cells were pre-treated with IST5-002 (1 h) and stimulated with IL-6 (50 ng/ml) (16 h). IST5-002 failed to block transcriptional activity of Stat3 (Fig. 2d) at a concentration that was highly effective at inhibiting Stat5a/b-driven transcription (Fig. 1e).

To assess the ability of IST5-002 to regulate the expression of Stat5a/b target genes in PC cells, CWR22Rv1 and LNCaP cells were treated with increasing concentrations of IST5-002 or Ctrl (48 h) (Fig. 2e), or a single dose of IST5-002 (25 μM) or Ctrl for the indicated times (Supplementary Fig. 5a). Immunoblotting of PC cell lysates showed that IST5-002 reduced expression of both Bcl-xL and cyclin D1 (Fig. 2e and Supplementary Fig. 5a), both previously demonstrated as Stat5a/b target genes in PC cells (2). We further assessed the

gene expression profiles induced by genetic (Stat5a/b shRNA) or pharmacological (IST5-002) knockdown of Stat5a/b in CML cells, as verified by immunoblotting (Fig. 2f). Genes (Supplementary Fig. 5b) regulated by both Stat5a/b-silencing and IST5-002 in CML cells are presented as Venn diagrams (Fig. 2f). The statistically significant ($p<0.01$) similarity between the gene expression changes induced by IST5-002 treatment and Stat5a/b knockdown in K562 cells indicate that these transcriptional changes are primarily due to loss of Stat5a/b activity and not to off-target effects (Fig. 2g, Supplementary Tables 2–5). Among known Stat5a/b target genes regulated by IST5-002 were Cyclin D2 (−2.3-fold), Pim1 (−1.7-fold), Pim2 (−1.7-fold), Myc (−1.7-fold), SOCS3 (−1.3-fold), CISH (−2.3-fold) and TRIB2 (−1.4-fold) (Supplementary Table 5). Gene ontology enrichment analysis revealed genes involved in metabolic processes, proliferation, processing of extracellular stimuli and remodeling actin cytoskeleton (Supplementary Fig. 5c).

IST5-002 suppresses Stat5a/b-mediated growth of PC through induction of apoptosis in experimental models of PC *in vitro*, *in vivo* and *ex vivo*

To investigate the effect of IST5-002 in PC cell growth, we treated three human PC cell lines with IST5-002 or Ctrl (72 h). In all three cell lines, IST5-002 decreased viable cells by 50–80% at 12.5 μM ($0<0.001$) (Fig. 3a). Treatment of CWR22Rv1 cells with 25 μM IST5-002 (24 h) resulted in a 5-fold increase in dead cells, as detected by trypan blue exclusion (Fig. 3b). In parallel wells, IST5-002 increased nucleosomal DNA fragmentation by 230%, suggesting that the mode of cell death was apoptotic ($p<0.001$) (Fig. 3c). IST5-002 (12.5 μM) induced a 3-fold increase in caspase-3 activation ($p<0.001$) (Fig. 3d). Importantly, overexpression of constitutively active Stat5a/b (3) by adenoviral vector (CAStat5a) 12 h prior to treatment with 12.5 μM IST5-002 prevented caspase-3 activation by IST5-002 (Fig. 3d). Cell cycle analysis of IST5-002- or Ctrl-treated (72 h) LNCaP and CWR22Rv1 cells revealed that IST5-002 increased the fraction of dead cells (sub-G1) and decreased the fraction of living cells (G2-M) (Fig. 3e). Treatment of CWR22Rv1 cells for 72 h with IST5-002 shows comparable efficacy to genetic knockdown of Stat5a/b by lentiviral transduction of Stat5a/b shRNA (Fig. 3f). Moreover, to test the effect of IST5-002 on the viability of PC cells after Stat5a/b had been genetically deleted, CWR22Rv1 cells were first transduced by lentiviral Stat5a/b shRNA vs. control shRNA for 24 h followed by treatment with IST5-002 for 48h. While IST5-002 (12.5 μM) induced 40% decrease in the number of viable PC cells expressing control shRNA, IST5-002 did not further affect viability of CWR22Rv1 cells depleted of Stat5a/b (shStat5a/b) (Fig. 3g). IST5-002 effects were PC-specific, as viability of malignant or immortalized cell lines originating from other tissues, including lung (A549), pancreas (CAPAN), breast (T47D), fibrosarcoma (HT1080), liver (HepG2) or monkey fibroblasts (COS-7), was not affected (Supplementary Figure 6a). When tested side-by-side, IST5-002 suppressed viability of PC (CWR22Rv1) and CML (K562) cells which both have high Stat5a/b activation, while IST5-002 did not affect viability of cell lines with low or no Stat5a/b activation (RC170N – normal prostate epithelial cell line; HT1080-fibrosarcoma cells) (Supplemetary Figure 6b).

To determine if IST5-002 efficacy extended to an *in vivo* model of PC, we inoculated CWR22Rv1 cells subcutaneously into the flanks of nude mice (Fig. 4a). Once PC xenograft tumors were established, mice were treated daily by intraperitoneal injection of IST5-002

(25, 50 or 100 mg/kg) or vehicle (hydroxypropyl cellulose, HPC). Tumor growth was significantly ($P<0.001$) suppressed in all IST5-002 treatment groups compared to the control groups (Fig. 4a, Supplementary Figure 7). IST5-002 induced massive loss of viable tumor cells and accumulation of dead rounded cells ($p<0.001$, IST5-002 groups vs. vehicle) (Fig. 4b). IST5-002 induced cell death through apoptosis, as shown by the presence of fragmented DNA in tumor sections (Supplementary Fig. 8a). IST5-002 decreased nuclear Stat5a/b content by 60%, 78% and 90% in groups treated with 25, 50 and 100 mg/kg, respectively, compared to vehicle (HPC) ($p<0.0001$) (Fig. 4c). Intratumor levels of nuclear Stat3 were not altered at any of the doses tested (Fig. 4d). Together, these results indicate that IST5-002 suppresses PC growth *in vitro* and *in vivo*, without general toxicity in normal prostate epithelial cells or solid tumor cells originating from other organs.

To evaluate efficacy of IST5-002 in clinical PC, we exploited an *ex vivo* organ explant culture system of patient-derived PCs from radical prostatectomies which we have previously established and characterized (4, 7, 34, 39). All tested clinical PCs (n=11) were of Gleason score 7 (Table 1), and were cultured for 7 days in the presence of IST5-002 or Ctrl at the indicated concentrations. Eight out of 11 patient-derived PCs responded to IST5-002 by extensive loss of viable epithelium, starting at 25 μM ($p=0.004$) (Fig. 4e). IST5-002 induced apoptotic death of explant epithelial cells in cancer acini, compared to explants cultured with Ctrl ($p=0.002$). Apoptosis was evidenced by accumulation of dead cells in acinar lumens (Supplementary Fig. 8b). Three out of 11 PCs did not show reduced epithelial cell viability in response to IST5-002 (Fig. 4e, right panel). Nuclear Stat5a/b contents showed a trend of down-regulation by IST5-002 in the 8 responsive PCs, but were lower and remained largely unaffected in the non-responsive PCs (Fig. 4f). To determine if Stat5a/b activation status could predict IST5-002 responsiveness in organ explant culture, we analyzed nuclear Stat5a/b levels in samples prior to culture. All non-responsive PCs had low or non-existent nuclear Stat5a/b expression, while nuclear Stat5a/b immunostaining was moderate or strong in all responsive PCs (Table 1). These results indicate that IST5-002 induces death of primary PC cells with high nuclear Stat5a/b expression.

IST5-002 inhibits Stat5a/b phosphorylation and induces apoptosis of imatinib-sensitive and -resistant CML cells

To determine IST5-002 efficacy in disrupting Stat5a/b phosphorylation in Bcr-Abl-driven leukemias, parental and imatinib-resistant CML cell lines (K562, KCL22 and BV173) were cultured for 24–72 h with increasing concentrations of IST5-002. IST5-002 potently inhibited Stat5a/b phosphorylation in both imatinib sensitive and -resistant CML cells (IC_{50}=2.5–7 μM) (Fig. 5a and 5b). Since Stat5a/b signaling is critical for Bcr-Abl-driven growth of CML cells, we investigated if IST5-002 affects viability of these cells. The number of living cells was assessed by trypan blue exclusion after treatment with IST5-002 (5 μM) for increasing periods of time (Fig. 5c), or by colony formation assay (Supplementary Fig. 9). In both assays, treatment with IST5-002 blocked the growth of imatinib-sensitive and -resistant CML cells. Cell cycle analysis of IST5-002-treated cells at 48 h showed an increase in apoptosis and a decrease in the fraction of G2-M or S-phase cells (Fig. 5d). Furthermore, IST5-002 decreased viability of acute lymphocytic leukemia cell line (ALL) (SUP-B15) which is driven by Bcr-Abl and has high Stat5a/b phosphorylation (Fig.

5e). At the same time, IST5-002 had only marginal or no effect on the viability of EBV-immortalized B-cells that express no active Stat5a/b (Fig. 5e). To evaluate IST5-002 efficacy in primary CML samples, cells obtained from three CML-chronic phase patients (n=3) were plated in methylcellulose in the presence of IST5-002 and colonies were counted after 7 days. In all three samples, IST5-002 suppressed cell growth, as indicated by the dramatic decrease in the number of viable colonies (Fig. 5f). In conclusion, IST5-002 potently inhibits Stat5a/b phosphorylation and growth of imatinib-sensitive and -resistant CML cells.

Discussion

While a critical role of Stat5a/b in pathogenesis of PC and myeloproliferative disorders has been established (1–22, 24), only a few pharmacological Stat5a/b inhibitors are currently available for clinical development (15, 42–44). In this work, we identified a potent lead compound Stat5a/b inhibitor, IST5-002, with high efficacy in abrogating Stat5a/b signaling in PC and CML. IST5-002 potently inhibited molecular events associated with Stat5a/b activation, reduced the expression of Stat5a/b-regulated genes and induced extensive apoptotic cell death in multiple models of PC and CML *in vitro*, *in vivo* in animal models and in patient samples.

Transcription factors are typically considered suboptimal pharmacological targets because their function relies on protein-protein and protein-DNA interactions that are not easily disrupted by small molecules. However, our strategy was to target the SH2-domain-phosphotyrosine interaction of cytoplasmic Stat5 as a signaling molecule, prior to phosphorylation, dimerization and nuclear translocation. While the structure of a fragment of unphosphorylated Stat5a-SH2 domain has been determined (36), this structure lacks the phosphotyrosyl bridge and, thus, is not useful for screening molecules to target Stat5a/b SH2-domain-pY interactions. We constructed a homology model of Stat5a/b SH2-domain based on the crystal structures of (2 h) phosphorylated Stats (30, 37). The lead compound Stat5 inhibitor, IST5-002, showed specificity for Stat5 over Stat3. This may be due to several reasons. First, the following Stat5a/b residues were selected as binding sites for *in-silico* screening: 600K, 604H, 618-RFSDSEIGG-626, 628T, 638-RMFWNLMPF-646, 707-VVPE-710. A comparison of these sites to the corresponding sequences in Stat3 reveals 15 differences, five of which are changes from hydrophobic (Stat5a/b) to charged (Stat3) amino acids. Moreover, the Stat3 sequence contains an inserted serine residue corresponding to a position between residues 622S and 623E in Stat5a/b. While the data presented in the present study provide evidence for IST5-002 inhibition of Stat5a/b phosphorylation and dimerization in multiple model systems, future work will need to evaluate if IST5-002 directly binds to the SH2-domain of Stat5a/b.

A number of nucleoside analogs structurally similar to IST5-002 (N6-benzyladenosine-5-monophosphate) (45) such as 2-chlorodeoxyadenosine, fludarabine, pentostatin and cladribine are currently in use as anti-cancer drugs (46, 47). Fludarabine was recently shown to inhibit Stat1 phosphorylation and activation but not affecting Stat5 activity (48). Analogous to fludarabine, IST5-002 inhibited molecular events involved in Stat5a/b activation while not affecting Stat3 activation. Moreover, IST5-002 induced extensive

apoptosis selectively in two cancers known to be driven by Stat5a/b, PC and CML, but was not generally cytotoxic to normal epithelial cells and affected only marginally the viability of other types of cancers not driven by Stat5a/b and with low or no Stat5a/b activation. While IST5-002 is a close derivative of AMP, AMP or similar mononucleotides such as GMP and cyclic AMP had no effect on Stat5a/b activation and transcriptional activity when tested side-by-side with IST5-002 (data not shown). The IC_{50} values of IST5-002 for suppression of transcriptional activity, phosphorylation, dimerization, nuclear translocation and viability varied between 1.5 μM and 22 μM. This is likely due to variability in the sensitivies of different assays as well as differences between cell lines in their dependence on Stat5 for survival.

Stat5a/b has been previously established as a candidate therapeutic target protein in prostate cancer (2, 4, 9, 20, 21). IST5-002 robustly inhibited viability of Jak2-Stat5a/b-driven PC cells in culture and growth of xenograft tumors in nude mice. Moreover, IST5-002 induced extensive epithelial cell death in the majority of 11 clinical PCs when tested *ex vivo* in organ explant cultures. Recently, pharmacological targeting of Stat5a/b by a Jak2 inhibitor, AZD1480, was shown to block growth of CRPC (4). Direct pharmacological inhibition of Stat5a/b is likely to target a larger fraction of clinical PCs than targeting the kinase, since Stat5a/b is a convergence point for multiple kinases in PC, including Jak2, Src and EGF-receptor family members (3, 31–35). Of note, positive status for active Stat5a/b in 11 clinical PCs predicted responsiveness to IST5-002 in *ex vivo* explant cultures, suggesting that Stat5a/b activation in PC biopsies could potentially serve as a biomarker for therapy selection.

IST5-002 induced extensive apoptotic death of both imatinib-sensitive and imatinib-resistant CML cells through potent inhibition of Stat5a/b. Moreover, IST5-002 blocked growth of primary CML-chronic phase cells. Current therapy for CML includes imatinib, dasatinib and nilotinib, which reduce Bcr-Abl kinase activity and Stat5a/b activation (49). Our data indicated high efficacy of IST5-002 suppressing growth of both imatinib-sensitive and imatinib-resistant CML cells. However, a key concern in CML therapy is the emergence of resistance to multiple kinase inhibitors, known to develop through Bcr-Abl point mutations (particularly T315I) (49) or overexpression. Pharmacological inhibition of Stat5a/b directly may provide an improved strategy for CML therapy, either after development of resistance to current kinase inhibitors or as a part of an initial combination therapy to prevent acquired resistance.

Supplementary Material

Refer to Web version on PubMed Central for supplementary material.

Acknowledgments

Financial Support

This work was supported by grants from NCI (2RO1CA11358-06 and 1R21CA178755-01 to M.T. Nevalainen and 1RO1CA167169-01 to B. Calabretta) and Pennsylvania Department of Health to M.T. Nevalainen, and Thomas Jefferson Univ. Intramural Funding (Dean’s Support for Programmatic Research Initiatives to M.T. Nevalainen, B.

Calabretta and G. Cingolani). Shared Resources of SKCC are partially supported by NIH Grant CA56036 (Cancer Center Support Grant, to SKCC).

References

1. Ahonen TJ, Xie J, LeBaron MJ, Zhu J, Nurmi M, Alanen K, et al. Inhibition of transcription factor Stat5 induces cell death of human prostate cancer cells. J Biol Chem. 2003; 278:27287–92. [PubMed: 12719422]
2. Dagvadorj A, Kirken RA, Leiby B, Karras J, Nevalainen MT. Transcription factor signal transducer and activator of transcription 5 promotes growth of human prostate cancer cells in vivo. Clin Cancer Res. 2008; 14:1317–24. [PubMed: 18316550]
3. Gu L, Dagvadorj A, Lutz J, Leiby B, Bonuccelli G, Lisanti MP, et al. Transcription factor Stat3 stimulates metastatic behavior of human prostate cancer cells in vivo, whereas Stat5b has a preferential role in the promotion of prostate cancer cell viability and tumor growth. Am J Pathol. 2010; 176:1959–72. [PubMed: 20167868]
4. Gu L, Liao Z, Hoang DT, Dagvadorj A, Gupta S, Blackmon S, et al. Pharmacologic Inhibition of Jak2-Stat5 Signaling By Jak2 Inhibitor AZD1480 Potently Suppresses Growth of Both Primary and Castrate-Resistant Prostate Cancer. Clin Cancer Res. 2013; 19:5658–74. [PubMed: 23942095]
5. Gu L, Vogiatzi P, Puhr M, Dagvadorj A, Lutz J, Ryder A, et al. Stat5 promotes metastatic behavior of human prostate cancer cells in vitro and in vivo. Endocr Relat Cancer. 2010; 17:481–93. [PubMed: 20233708]
6. Haddad BR, Gu L, Mirtti T, Dagvadorj A, Bajaj R, Vogiatzi P, et al. Stat5a/b gene locus undergoes amplification during human prostate cancer progression. Am J Pathol. 2013; 182:2264–2275. [PubMed: 23660011]
7. Li H, Ahonen TJ, Alanen K, Xie J, LeBaron MJ, Pretlow TG, et al. Activation of signal transducer and activator of transcription 5 in human prostate cancer is associated with high histological grade. Cancer Res. 2004; 64:4774–82. [PubMed: 15256446]
8. Li H, Zhang Y, Glass A, Zellweger T, Gehan E, Bubendorf L, et al. Activation of signal transducer and activator of transcription-5 in prostate cancer predicts early recurrence. Clin Cancer Res. 2005; 11:5863–8. [PubMed: 16115927]
9. Thomas C, Zoubeidi A, Kuruma H, Fazli L, Lamoureux F, Beraldi E, et al. Transcription factor Stat5 knockdown enhances androgen receptor degradation and delays castration-resistant prostate cancer progression in vivo. Molecular cancer therapeutics. 2010; 10:347–59. [PubMed: 21216933]
10. Casetti L, Martin-Lanneree S, Najjar I, Plo I, Auge S, Roy L, et al. Differential contributions of STAT5A and STAT5B to stress protection and tyrosine kinase inhibitor resistance of chronic myeloid leukemia stem/progenitor cells. Cancer Res. 2013; 73:2052–8. [PubMed: 23400594]
11. de Groot RP, Raaijmakers JA, Lammers JW, Jove R, Koenderman L. STAT5 activation by BCR-Abl contributes to transformation of K562 leukemia cells. Blood. 1999; 94:1108–12. [PubMed: 10419904]
12. Hoelbl A, Schuster C, Kovacic B, Zhu B, Wickre M, Hoelzl MA, et al. Stat5 is indispensable for the maintenance of bcr/abl-positive leukaemia. EMBO Mol Med. 2010; 2:98–110. [PubMed: 20201032]
13. Horita M, Andreu EJ, Benito A, Arbona C, Sanz C, Benet I, et al. Blockade of the Bcr-Abl kinase activity induces apoptosis of chronic myelogenous leukemia cells by suppressing signal transducer and activator of transcription 5-dependent expression of Bcl-xL. J Exp Med. 2000; 191:977–84. [PubMed: 10727459]
14. Lin TS, Mahajan S, Frank DA. STAT signaling in the pathogenesis and treatment of leukemias. Oncogene. 2000; 19:2496–504. [PubMed: 10851048]
15. Nelson EA, Walker SR, Weisberg E, Bar-Natan M, Barrett R, Gashin LB, et al. The STAT5 inhibitor pimozide decreases survival of chronic myelogenous leukemia cells resistant to kinase inhibitors. Blood. 2011; 117:3421–9. [PubMed: 21233313]
16. Nieborowska-Skorska M, Wasik MA, Slupianek A, Salomoni P, Kitamura T, Calabretta B, et al. Signal transducer and activator of transcription (STAT)5 activation by BCR/ABL is dependent on intact Src homology (SH)3 and SH2 domains of BCR/ABL and is required for leukemogenesis. J Exp Med. 1999; 189:1229–42. [PubMed: 10209040]

17. Soliera AR, Mariani SA, Audia A, Lidonnici MR, Addya S, Ferrari-Amorotti G, et al. Gfi-1 inhibits proliferation and colony formation of p210BCR/ABL-expressing cells via transcriptional repression of STAT 5 and Mcl-1. Leukemia. 2012; 26:1555–63. [PubMed: 22285998]
18. Warsch W, Kollmann K, Eckelhart E, Fajmann S, Cerny-Reiterer S, Holbl A, et al. High STAT5 levels mediate imatinib resistance and indicate disease progression in chronic myeloid leukemia. Blood. 2011; 117:3409–20. [PubMed: 21220747]
19. Ye D, Wolff N, Li L, Zhang S, Ilaria RL Jr. STAT5 signaling is required for the efficient induction and maintenance of CML in mice. Blood. 2006; 107:4917–25. [PubMed: 16522816]
20. Ahonen TJ, Harkonen PL, Laine J, Rui H, Martikainen PM, Nevalainen MT. Prolactin is a survival factor for androgen-deprived rat dorsal and lateral prostate epithelium in organ culture. Endocrinology. 1999; 140:5412–21. [PubMed: 10537173]
21. Mirtti T, Leiby BE, Abdulghani J, Aaltonen E, Pavela M, Mamtani A, et al. Nuclear Stat5a/b predicts early recurrence and prostate cancer-specific death in patients treated by radical prostatectomy. Hum Pathol. 2013; 44:310–9. [PubMed: 23026195]
22. Kazansky AV, Spencer DM, Greenberg NM. Activation of signal transducer and activator of transcription 5 is required for progression of autochthonous prostate cancer: evidence from the transgenic adenocarcinoma of the mouse prostate system. Cancer Res. 2003; 63:8757–62. [PubMed: 14695191]
23. Tan SH, Dagvadorj A, Shen F, Gu L, Liao Z, Abdulghani J, et al. Transcription factor Stat5 synergizes with androgen receptor in prostate cancer cells. Cancer Res. 2008; 68:236–48. [PubMed: 18172316]
24. Daley GQ, Van Etten RA, Baltimore D. Induction of chronic myelogenous leukemia in mice by the P210bcr/abl gene of the Philadelphia chromosome. Science. 1990; 247:824–30. [PubMed: 2406902]
25. Gesbert F, Griffin JD. Bcr/Abl activates transcription of the Bcl-X gene through STAT5. Blood. 2000; 96:2269–76. [PubMed: 10979976]
26. Savage DG, Antman KH. Imatinib mesylate--a new oral targeted therapy. N Engl J Med. 2002; 346:683–93. [PubMed: 11870247]
27. Branford S, Rudzki Z, Walsh S, Grigg A, Arthur C, Taylor K, et al. High frequency of point mutations clustered within the adenosine triphosphate-binding region of BCR/ABL in patients with chronic myeloid leukemia or Ph-positive acute lymphoblastic leukemia who develop imatinib (STI571) resistance. Blood. 2002; 99:3472–5. [PubMed: 11964322]
28. Gorre ME, Mohammed M, Ellwood K, Hsu N, Paquette R, Rao PN, et al. Clinical resistance to STI-571 cancer therapy caused by BCR-ABL gene mutation or amplification. Science. 2001; 293:876–80. [PubMed: 11423618]
29. Levy DE, Darnell JE Jr. Stats: transcriptional control and biological impact. Nat Rev Mol Cell Biol. 2002; 3:651–62. [PubMed: 12209125]
30. Becker S, Groner B, Muller CW. Three-dimensional structure of the Stat3beta homodimer bound to DNA. Nature. 1998; 394:145–51. [PubMed: 9671298]
31. Dagvadorj A, Collins S, Jomain JB, Abdulghani J, Karras J, Zellweger T, et al. Autocrine prolactin promotes prostate cancer cell growth via Janus kinase-2-signal transducer and activator of transcription-5a/b signaling pathway. Endocrinology. 2007; 148:3089–101. [PubMed: 17412813]
32. Feldman L, Wang Y, Rhim JS, Bhattacharya N, Loda M, Sytkowski AJ. Erythropoietin stimulates growth and STAT5 phosphorylation in human prostate epithelial and prostate cancer cells. Prostate. 2006; 66:135–45. [PubMed: 16161153]
33. Giri D, Ozen M, Ittmann M. Interleukin-6 is an autocrine growth factor in human prostate cancer. Am J Pathol. 2001; 159:2159–65. [PubMed: 11733366]
34. Nevalainen MT, Valve EM, Ingleton PM, Nurmi M, Martikainen PM, Harkonen PL. Prolactin and prolactin receptors are expressed and functioning in human prostate. J Clin Invest. 1997; 99:618–27. [PubMed: 9045863]
35. Hantschel O, Warsch W, Eckelhart E, Kaupe I, Grebien F, Wagner KU, et al. BCR-ABL uncouples canonical JAK2-STAT5 signaling in chronic myeloid leukemia. Nat Chem Biol. 2012; 8:285–93. [PubMed: 22286129]

36. Neculai D, Neculai AM, Verrier S, Straub K, Klumpp K, Pfitzner E, et al. Structure of the unphosphorylated STAT5a dimer. J Biol Chem. 2005; 280:40782–7. [PubMed: 16192273]
37. Chen X, Vinkemeier U, Zhao Y, Jeruzalmi D, Darnell JE Jr, Kuriyan J. Crystal structure of a tyrosine phosphorylated STAT-1 dimer bound to DNA. Cell. 1998; 93:827–39. [PubMed: 9630226]
38. Onishi M, Nosaka T, Misawa K, Mui AL, Gorman D, McMahon M, et al. Identification and characterization of a constitutively active STAT5 mutant that promotes cell proliferation. Mol Cell Biol. 1998; 18:3871–9. [PubMed: 9632771]
39. Nevalainen MT, Harkonen PL, Valve EM, Ping W, Nurmi M, Martikainen PM. Hormone regulation of human prostate in organ culture. Cancer Res. 1993; 53:5199–207. [PubMed: 7693334]
40. Berger A, Hoelbl-Kovacic A, Bourgeais J, Hoefling L, Warsch W, Grundschober E, et al. PAK-dependent STAT5 serine phosphorylation is required for BCR-ABL-induced leukemogenesis. Leukemia. 2014; 28:629–41. [PubMed: 24263804]
41. Hedvat M, Huszar D, Herrmann A, Gozgit JM, Schroeder A, Sheehy A, et al. The JAK2 inhibitor AZD1480 potently blocks Stat3 signaling and oncogenesis in solid tumors. Cancer Cell. 2009; 16:487–97. [PubMed: 19962667]
42. Muller J, Sperl B, Reindl W, Kiessling A, Berg T. Discovery of chromone-based inhibitors of the transcription factor STAT5. Chembiochem. 2008; 9:723–7. [PubMed: 18247434]
43. Nam S, Scuto A, Yang F, Chen W, Park S, Yoo HS, et al. Indirubin derivatives induce apoptosis of chronic myelogenous leukemia cells involving inhibition of Stat5 signaling. Mol Oncol. 2012; 6:276–83. [PubMed: 22387217]
44. Page BD, Khoury H, Laister RC, Fletcher S, Vellozo M, Manzoli A, et al. Small molecule STAT5-SH2 domain inhibitors exhibit potent antileukemia activity. J Med Chem. 2012; 55:1047–55. [PubMed: 22148584]
45. Catane R, Kaufman JH, Nime FA, Evans JT, Mittelman A. Phase I study of N6-benzyladenosine-5′-monophosphate. Cancer Treat Rep. 1978; 62:1371–3. [PubMed: 688280]
46. Hallek M. Chronic lymphocytic leukemia: 2013 update on diagnosis, risk stratification and treatment. Am J Hematol. 2013; 88:803–16. [PubMed: 23720127]
47. Robak P, Robak T. Older and new purine nucleoside analogs for patients with acute leukemias. Cancer Treat Rev. 2013; 39:851–61. [PubMed: 23566572]
48. Torella D, Curcio A, Gasparri C, Galuppo V, De Serio D, Surace FC, et al. Fludarabine prevents smooth muscle proliferation in vitro and neointimal hyperplasia in vivo through specific inhibition of STAT-1 activation. Am J Physiol Heart Circ Physiol. 2007; 292:H2935–43. [PubMed: 17293493]
49. Goldman JM, Melo JV. Targeting the BCR-ABL tyrosine kinase in chronic myeloid leukemia. N Engl J Med. 2001; 344:1084–6. [PubMed: 11287980]

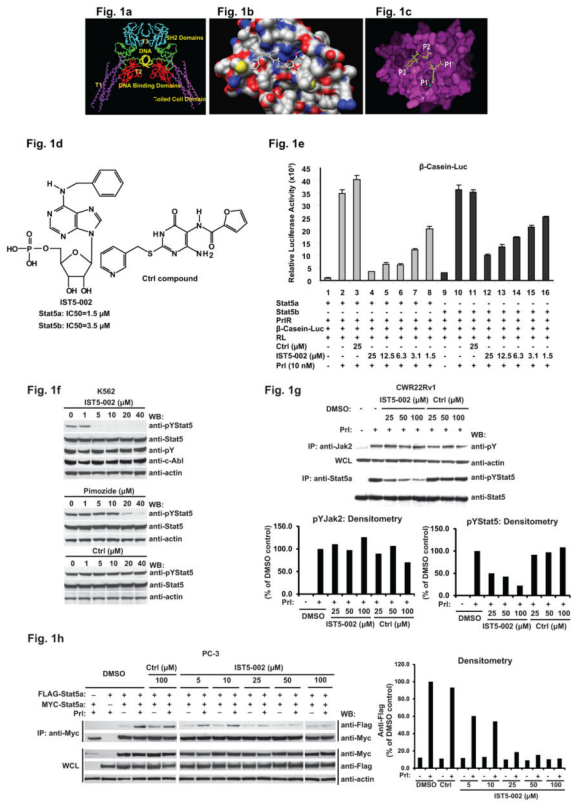

Figure 1. Identification and functional characterization of the Stat5a/b inhibitor IST5-002

(a) Ribbon presentation of the crystal structure of Stat-DNA complex and the various functional domains are labeled. **(b)** Predicted binding model of IST5-002 to the Stat5a SH2-domain, shown as atom-based (carbon: white, oxygen: red, nitrogen: blue, phosphorous: cyan, sulfur: yellow) bonds within the binding site at the SH2 dimer interface, and by **(c)** stick model, depicting the SH2 dimer interface site of Stat5a (magenta) with labeled sub-pockets P1, P2, P3 and P1′ of the SH2 interface. **(d)** Chemical structures of the Stat5a/b inhibitor IST5-002 and the control compound (Ctrl) with similar molecular weight as IST5-002. **(e)** IST5-002 inhibits transcriptional activity of Stat5a/b. PC-3 cells were transiently co-transfected with a β-casein-promoter-luciferase plasmid, pRL-TK (*Renilla* luciferase), pPrl-receptor (PrlR), pStat5a or pStat5b, as indicated. Cells were serum-starved (0% FBS) (10 h) and pre-treated with IST5-002 or Ctrl at the indicated concentrations (2 h), followed by stimulation with 10 nM human prolactin (hPrl) (16 h). Relative luciferase activities were determined, and mean values of three independent experiments performed in triplicate ± S.E. values are indicated by bars. **(f, g)** IST5-002 inhibits Bcr-Abl-driven **(f)** and Jak2-driven **(g)** Stat5 phosphorylation. Whole cell lysates of exponentially growing K562 cells and Stat5a/b immunoprecipitates of CWR22Rv1 cells were immunoblotted with anti-pYStat5 mAb, anti-Stat5a/b mAb, anti-pY mAb (for Jak2), anti-c-Abl pAb or anti-actin pAb as loading control. In CWR22Rv1 cells, Stat5 and Jak2 were immunoprecipitated using anti-Stat5a or anti-Jak2 pAbs from serum-starved CWR22Rv1 cells (16 h), treated with IST5-002 (2 h), followed by stimulation with 10 nM hPrl (30 min). **(h)** IST5-002 suppresses Stat5 dimerization. pCMV-3Flag-Stat5a, pCMV-3Mys-Stat5a and pPrlR plasmids were co-

transfected into PC-3 cells. Cells were serum-starved (16 h), pre-treated with IST5-002 or Ctrl at indicated concentrations (2 h), followed by stimulation with 10 nM hPrl (30 min). 3-Myc-Stat5a was immunoprecipitated with anti-Myc mAb and blotted with anti-Flag mAb or anti-Myc mAb, as indicated. Whole cell lysates were blotted with anti-Myc, anti-Flag mAb or anti-actin pAb to demonstrate the input.

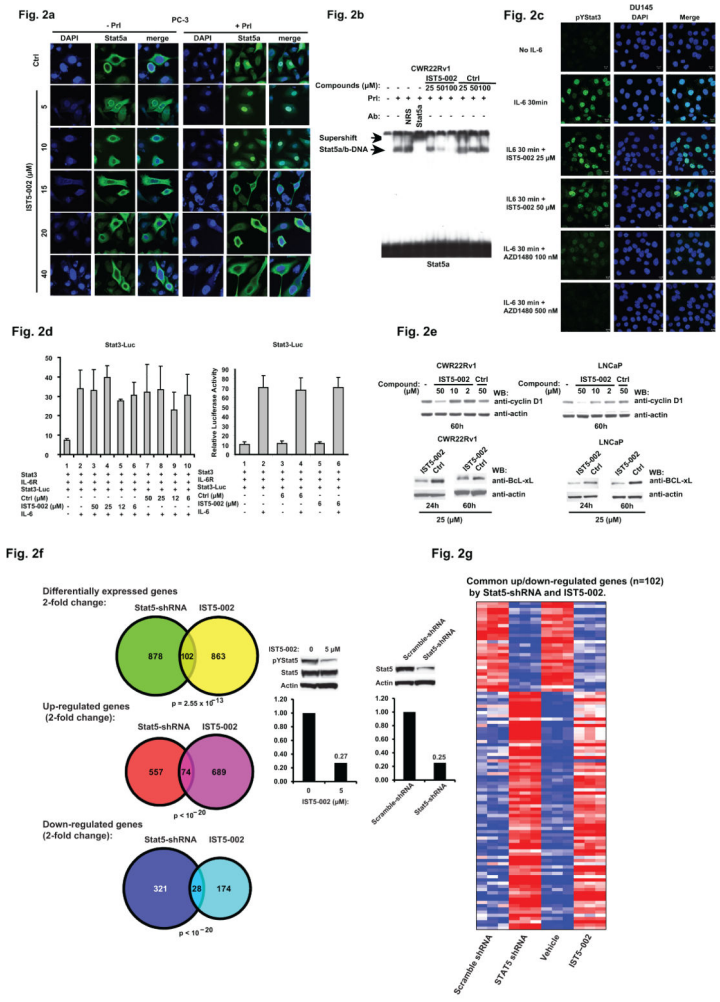

Figure 2. IST5-002 inhibits Stat5 nuclear translocation, DNA binding and expression of Stat5 target genes

(**a**) IST5-002 inhibits Prl-induced nuclear translocation of Stat5 in PC cells. PC-3 cells were infected with adenoviruses expressing wild-type Stat5a (AdWTStat5a; MOI=4) and human Prl-receptor (AdPrlR; MOI=4). Serum-starved (16 h) cells were treated with IST5-002 or Ctrl (2 h), followed by stimulation with 10 nM hPrl (30 min). Immunostaining of Stat5 is demonstrated by indirect immunofluoresence (green), while DAPI staining (blue) shows the nuclei. (**b**) IST5-002 inhibits binding of Stat5 to DNA shown by EMSA analysis using the Stat5-response element of beta-casein gene as the probe. COS-7 cells were transiently co-transfected with pStat5a and pPrlR, serum-starved (10 h) and treated with IST5-002 or Ctrl at indicated concentrations (2 h) followed by stimulation with 10 nM hPrl (30 min). The specificity of the Stat5-DNA binding complex was demonstrated by supershift with anti-Stat5a pAb vs. normal rabbit serum (NRS). **(c)** IST5-002 does not inhibit nuclear translocation of Stat3 in PC cells. Serum-starved DU145 cells were pretreated with IST5-002, AZD1480 or vehicle (2 h) before stimulation with 5 nM IL-6 (30 min). Immunostaining of Stat3 is demonstrated by indirect immunofluoresence (green), while DAPI staining (blue) shows the nuclei. **(d)** IST5-002 does not inhibit transcriptional activity of Stat3 in PC cells. LNCaP cells were transiently co-transfected with pStat3, pIL-6-receptor

(pIL-6R), pStat3-Luc and pRL-TK (*Renilla* luciferase). Cells were serum-starved (10 h), pre-treated with 6.0 μM IST5-002 or Ctrl (2 h), followed by stimulation with 50 ng/ml IL-6 (16 h). Relative luciferase activities were determined, and mean values of three independent experiments performed in triplicate ± S.E. values are indicated by bars. (**e**) IST5-002 downregulates the expression of Stat5 target genes cyclin D1 and Bcl-xL in PC cells. Exponentially growing CWR22Rv1 and LNCaP cells were treated with IST5-002 or Ctrl and whole cell lysates were immunoblotted with anti-cyclinD1 mAb or anti-Bcl-xL pAb. **(f)** Expression profiling of genes regulated by both genetic knockdown of Stat5 and IST5-002 in CML cells. Stat5 was suppressed in K562 cells by lentiviral expression of Stat5 shRNA vs. scramble control for 6 days or by treatment of the cells with IST5-002 (5 μM) for 48 h. Venn-diagrams of Stat5-shRNA and/or IST5-002 regulated genes in K562 cells meeting criteria for significant up/down-regulation (FDR-adjusted P-value < 0.05, >2-fold change) (left). Inhibition of Stat5 protein expression and phosphorylation demonstrated by immunoblotting of whole cell lysates with anti-pYStat5 mAb and anti-Stat5 mAb vs. anti-actin pAb as loading control (right). **(g)** The heatmap represents patterns of differential expression for 102 genes (listed in Supplementary Table 2) significantly regulated by both Stat5 knockdown and IST5-002. Red represents higher expression, whereas blue represents lower expression.

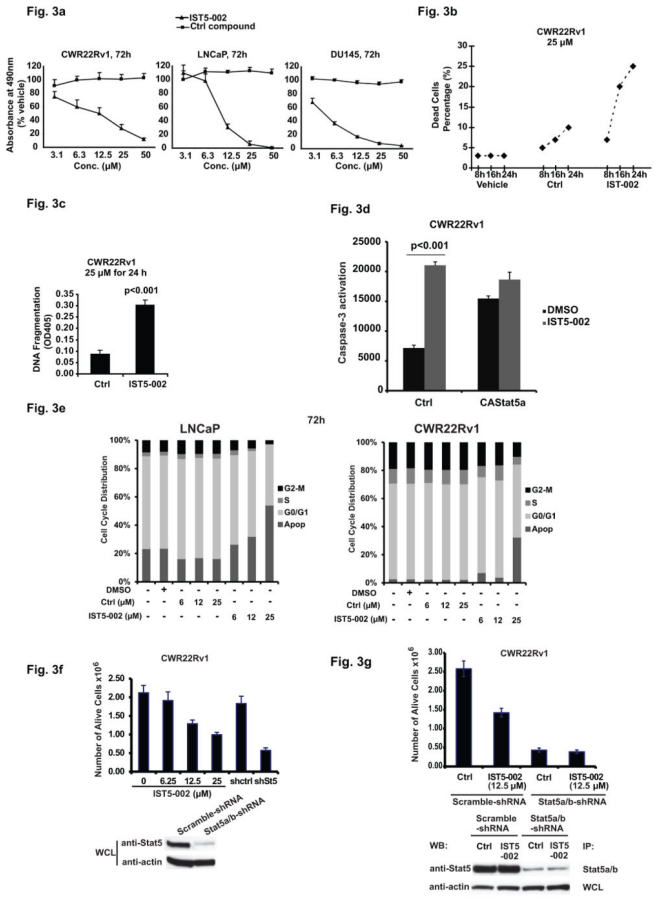

Figure 3. IST5-002 decreases viability of human PC cells *in vitro.*

(a) CWR22Rv1, LNCaP and DU145 cells were treated with IST5-002, Ctrl or vehicle, and the fraction of living cells was determined by MTS (3-(4,5-dimethylthiazolyl-2)-2,5-diphenyl-tetrazolium bromide) metabolic activity assay. **(b)** CWR22Rv1 cells were treated with 25 μM IST5-002, Ctrl or vehicle (24 h) followed by trypan blue exclusion and dead cells were manually counted. **(c)** In parallel wells, nucleosomal DNA fragmentation, indicating cell death due to apoptosis, was demonstrated by nucleosomal ELISA at 405 nm. **(d)** IST5-002 induces an increase in caspase-3 activation in CWR22Rv1 cells (72 h) ($p<0.001$), which was counteracted by expression of constitutively active (CA) Stat5a/b. CWR22Rv1 cells were infected with adenovirus expressing CAStat5a (AdCAStat5a; MOI=2) 12 h prior to treatment of cells with IST5-002 (12 μM) or vehicle, followed by determination of caspase-3 activation by fluorometric immunosorbent enzyme assay. **(e)** IST5-002 increases the fraction of dead PC cells in cell cycle analysis. LNCaP and CWR22Rv1 cells were treated with IST5-002 or Ctrl for 72 h at indicated concentrations followed by FACS analysis. (**f**) CWR22Rv1 cells were treated with IST5-002 at indicated concentrations or transduced with lentiviral shStat5a/b (Stat5a/b-shRNA) or control shRNA (scramble-shRNA) for 72 h and alive cells were counted manually after trypan blue exclusion. **(g)** To test the effect of IST5-002 on prostate cancer cell viability after genetic knockdown of Stat5a/b, CWR22Rv1 cells were first transduced with lentiviral Stat5a/b shRNA (Stat5a/b-shRNA) or control shRNA (scramble-shRNA). After 24 h, the cells were

treated with IST5-002 (12.5 μM) or control compound (Ctrl) for 48h and alive cells were counted manually after trypan blue exclusion.

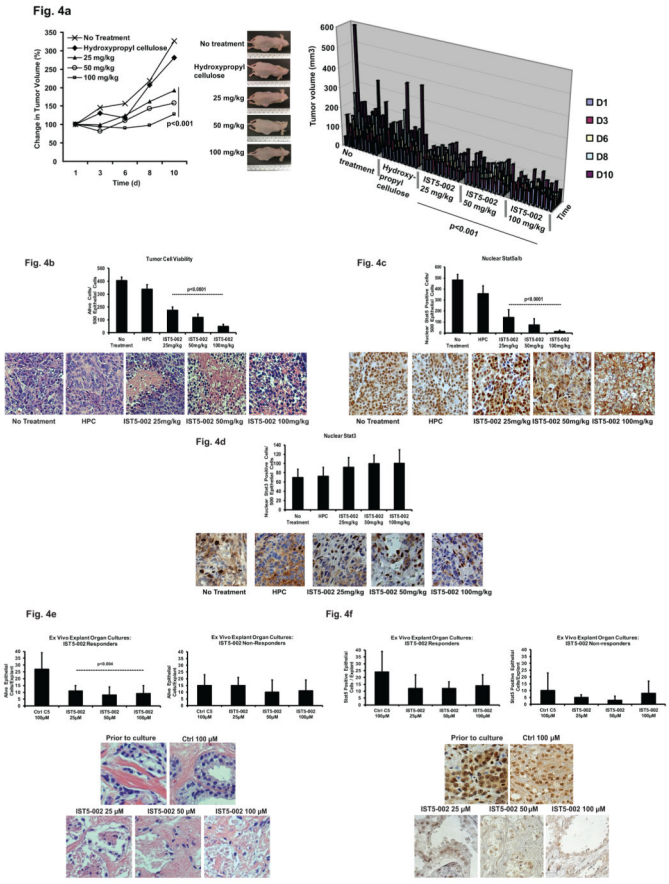

Figure 4. IST5-002 inhibits PC xenograft tumor growth *in vivo* in nude mice and induces death of epithelial cells in patient-derived PCs *ex vivo* in organ explant cultures

(**a**) CWR22Rv1 PC cells were inoculated subcutaneously into the flanks of castrated athymic nude mice supplied with sustained-release 5α-dihydrotestosterone (DHT)-pellets (n=10/group, 1 tumor/mouse, 1.5×10^7 CWR22Rv1 cells per site, 1 DHT pellet/mouse). Mice were treated with IST5-002 (25, 50 and 100 mg/kg) or vehicle (hydroxypropyl cellulose; HPC) as control intraperitoneally (i.p.) daily, with a group with no treatment as an additional control. Tumor sizes were measured every 3 days, and tumor volumes were calculated using the formula $V= (\pi/6) \times d_1 \times (d_2)^2$, with d_1 and d_2 being two perpendicular tumor diameters. Columns represent % change in tumor volume and growth of individual tumors. Tumor growth was significantly ($p<0.001$) suppressed in all IST5-002 treatment groups compared to the control groups. **(b)** IST5-002 induces apoptotic cell death in CWR22Rv1 PC xenograft tumors. Hematoxylin-eosin staining of the sections demonstrates loss of viable tumor cells and accumulation of dead cells (arrows) in IST5-002-treated CWR22Rv1 xenograft tumors vs. controls. **(c)** Immunostaining of nuclear active Stat5a/b or **(d)** Stat3 of paraffin-embedded sections of the prostate xenograft tumors. **(e)** To test responsiveness of primary PCs to IST5-002, 11 localized PCs (Table 1) were cultured for 7 days *ex vivo* as explant organ cultures in basal medium in the presence of IST5-002 at indicated concentrations or Ctrl. Eight PCs showed loss of viable acinar epithelium in response to IST5-002 (responders, left panel), while in three PCs, epithelial viability remained intact after IST5-002 treatment (non-responders, right panel). Representative

histology of an individual PC that responded to IST5-002 with extensive loss of acinar epithelium **(f).** Immunodetection shows intense positive immunostaining for nuclear Stat5 in explants cultured in the presence of Ctrl, while IST5-002 reduced levels of nuclear Stat5 expression. Representative immunostaining of nuclear Stat5 in a PC that responded to IST5-002 is presented.

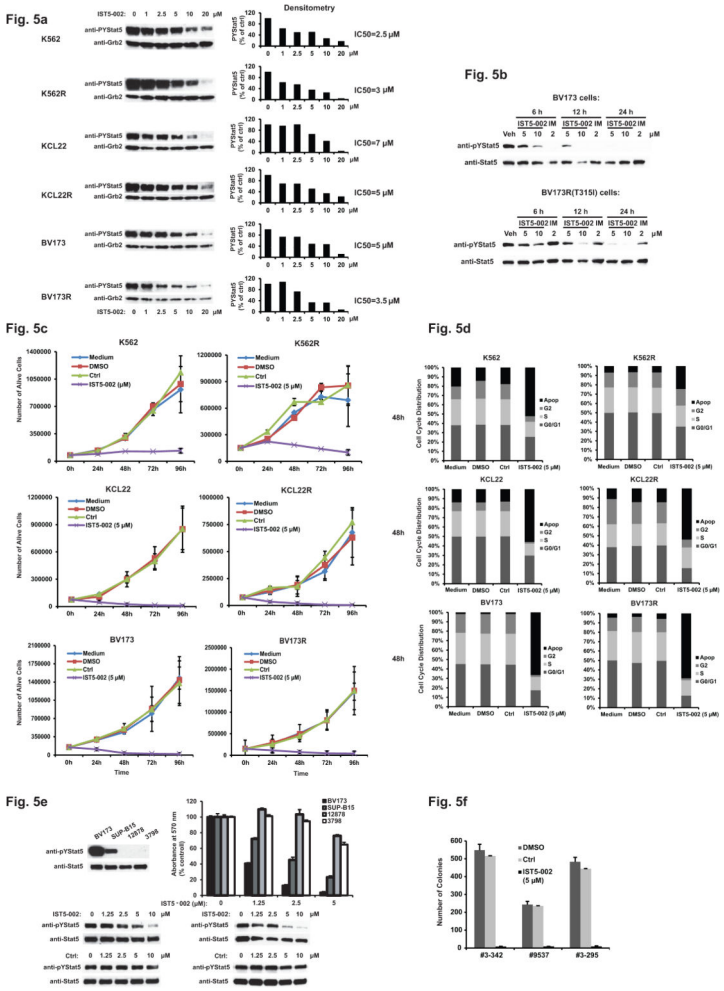

Figure 5. IST5-002 inhibits Stat5 phosphorylation and induces extensive apoptotic death of imatinib-sensitive and -resistant CML cells

(a) Western blotting (left) and densitometry (right) showing the levels of phosphorylated Stat5a/b in IST5-002-treated (12 h) parental (sensitive) and imatinib-resistant KCL22, K562 and BV173 cells. Grb2 levels were monitored as loading control. **(b)** Western blot of phosphorylated Stat5a/b levels in imatinib-sensitive or –resistant (T315I) BV173 cells treated with IST5-002 or imatinib at the indicated concentrations for 6, 12 or 24 h. **(c)** Cell counts (trypan blue exclusion) of IST5-002-treated (5 μM) imatinib-sensitive and imatinib-resistant CML blast crisis cell lines; **(d)** Cell cycle distribution of control (medium, DMSO, or Ctrl) or IST5-002-treated (5 μM) CML-blast crisis cell lines; **(e)** IST5-002 decreases viability of Bcr-Abl-driven lymphoid blast crisis cells (BV173) and acute lymphocytic leukemia cells (SUP-B15) with high Stat5 activation, while having marginal effect on EBV-immortalized B cells with no Stat5a/b activation (12878, 3798). Levels of STAT5 phosphorylation of Bcr-Abl expressing BV173 and SUP-B15 cell lines, and Bcr-Abl negative, EBV immortalized 12878 and 3798 B-cell lines (upper left panel). Cell viability (MTT assay) of IST5-002-treated (48 h) BV173, SUP-B15, 12878 and 3798 cell lines (upper right panel). Levels of STAT5 phosphorylation of SUP-B15 and BV173 after 12 hours of treatment with IST5-005 or Ctrl at the indicated concentrations (lower panels). **(f)** Colony

formation of IST5-002-treated primary CML-chronic phase cells from patients. Colonies were counted 9 days after plating and the results are expressed as % colony formation inhibition of treated vs. untreated cells.

Table 1

Prostate cancers cultured ex vivo in explant organ cultures.

Age at the day of operation	Gleason grade	Gleason score	Stage	Nuclear Stat5levels
58	(3+4)	7	T3a	3
66	(4+3)	7	T2b	3
72	(4+3)	7	T1c	3
55	(3+4)	7	T2b	3
66	(3+4)	7	T1c	2
60	(3+4)	7	T2a	2
55	(3+4)	7	T2a	3
67	(3+4)	7	T2a	2
*50	(3+4)	7	T2b	1
*65	(4+3)	7	T2c	1
*66	(4+3)	7	T3a	0

Ages of the patients ranged from 50 to 72 years at the time of the operation (mean age 62 yrs). Asterisk indicates PC samples which did not respond to IST5-002 by cancer cell death. Samples of each prostate cancer were scored for nuclear Stat5 levels on a scale from 0 to 3 where 0 represented negative, 1 weak, 2 moderate and 3 strong immunostaining.